Polymer 49 (2008) 4819–4825

Contents lists available at ScienceDirect

Polymer

journal homepage: www.elsevier.com/locate/polymer

Aggregation behavior of new cyclic saturated copolymers synthesized *via* ring-opening metathesis polymerization

Yoichi Ogata [a,*], Yutaka Makita [b], Motoki Okaniwa [c]

[a] *Advanced Lithography Research Group, JSR Micro, Inc., 1280 North Mathilda Avenue, Sunnyvale, CA 94089, United States*
[b] *Material Characterization and Analysis Laboratory, Yokkaichi Research Center, JSR Corporation, 100 Kawajiri-cho, Yokkaichi, Mie 510-8552, Japan*
[c] *Performance Polymers Laboratory, Performance Materials Research Laboratory, Yokkaichi Research Center, JSR Corporation, 100 Kawajiri-cho, Yokkaichi, Mie 510-8552, Japan*

ARTICLE INFO

Article history:
Received 21 May 2008
Received in revised form 27 August 2008
Accepted 29 August 2008
Available online 9 September 2008

Keywords:
Ring-opening metathesis polymerization
Dynamic light scattering
Aggregation

ABSTRACT

Cyclic saturated copolymers were prepared from 8-methyl-8-methoxycarbonyltetracyclo[4.4.0.1^{2,5}.1^{7,10}]dodec-3-ene (MMT) with polar ester group and dicyclopentadiene (DCP) without polar group. This procedure consisted of ring-opening metathesis polymerization (ROMP) followed by hydrogenation. Monomer reactivity of DCP was higher than that of MMT; the monomer reactivity ratio r_{DCP}/r_{MMT} varied from 2.135 to 1.159 in a temperature range from 80 to 130 °C. These kinetic results indicated that the copolymer had distribution of DCP composition in a macromolecule chain, which could provide the interesting aggregation behavior. The aggregation behaviors of the hydrogenated copolymer and the homopolymer in various solvents were also examined using dynamic light scattering (DLS) and static light scattering (SLS). DLS analysis indicated that the fast mode in each polymer is attributed to the diffusive motion of each single polymer chain, while the slow mode in the copolymer is caused by aggregated polymer. The aggregation degree of the copolymer decreased with increasing hydrophobicity of solvent, decreasing polymer concentration, decreasing molecular size of solvent and increasing temperature. Based on these findings, the mechanism of aggregation behavior was clarified that the DCP-rich unit in a macromolecule might be acting as core to give the aggregation in poor solvent.

1. Introduction

Polymer behavior in solution is highly complex because polymers can take varied forms due to the large size compared with low molecular weight compounds. Additionally, polymers have interesting correlations between solubility and aggregation in solution. For example, polymer solubility is greatly affected by the affinity between polymer and solvent. The driving force for aggregation is a decrease of the polymer solubility, which can result from intramolecular or intermolecular interactions such as hydrogen-bonding, ion-related electrostatic interactions and ligand–metal coordination [1–13]. Topuza et al. demonstrated interactions between functional groups and a temperature dependence in forming polymer complexes between polystyrene-*b*-poly(2-vinylpyridine) and poly(methacrylic acid) in dioxane using light-scattering measurement and viscosity measurement [2]. The relationship between polymer solubility and aggregate formation has prominently been reported in cellulose [3–5], amphiphilic micelle [6,7] and salt addition [8–10]. The solubility of alkali-soluble emulsion polymer controls the conformational transition from a compact sphere to a random coil during the process of neutralization [11]. As for poly(2,5-difluoraniline) [12] and poly(aryleneethynylene) [13], the substituent effect on solubility or aggregation has been reported.

Ring-opening metathesis polymerization (ROMP) is a widespread tool to synthesize well-defined and highly functionalized polymer. JSR Corporation has been developing hydrogenated cyclic olefin polymers under the trade name of ARTON prepared from 8-methyl-8-methoxycarbonyltetracyclo[4.4.0.1^{2,5}.1^{7,10}]dodec-3-ene (MMT) *via* ROMP. ARTON exhibits quite high glass transition temperature, i.e., 171 °C, and high transparency and shows anisotropic nature of the bulky cyclic chain sticking out of the main chain, which will compensate birefringence caused by main-chain orientation and should contribute to low birefringence of the resulting polymer [14,15]. In other words, ARTON provides excellent properties as optical polymer. Optical polymer is now being used extensively for versatile applications such as optical lens, optical disk and liquid crystal display because of its light-weight, break-proof, modability and optical characteristic as typified by high transparency and easiness to generate

* Corresponding author. Tel.: +1 510 486 7691; fax: +1 408 543 8996.
E-mail address: yogata@jsrmicro.com (Y. Ogata).

0032-3861/$ – see front matter © 2008 Elsevier Ltd. All rights reserved.
doi:10.1016/j.polymer.2008.08.047

birefringence. On the other hand, a copolymer, which is aimed at performance advances as optical polymer, exhibits a singular phenomenon, meaning aggregation in specific solvents unlike homopolymer such as ARTON. The aggregation behavior is extremely interesting in polymer solution property.

In this article, we report the synthesis and properties of new cyclic saturated copolymer prepared from MMT and dicyclopentadine (DCP). The behavior of copolymer consisting of both polar monomer and non-polar monomer differs significantly from the homopolymer consisting of a polar monomer. Aggregation could be depressed by selection of solvent, i.e., mixed solvent composed of toluene (TL) and cyclopentene (CPE), as well as increasing heating temperature in mixed solvent consisting of TL and cyclohexane (CHX). Aggregation on the micrometer size order inhibits optical application of new materials because optical materials require a filtration process to remove particles in submicron size-range. We believe that resolution of the aggregation mechanism and finding conditions without aggregation will offer interesting possibilities for applications in industrial large scale production of new optical materials.

2. Experimental

2.1. Materials

Toluene and DCP (Maruzen chemical) were dried over molecular sieves (type 4 A) under nitrogen. MMT (JSR) was freshly distilled before use. The other reagents were obtained commercially and used as received.

2.2. Syntheses of the homopolymer and the copolymer

In a 500 mL autoclave purged with dry nitrogen fitted with a stirrer were placed 25 g DCP (0.189 mol), 75 g MMT (0.323 mol), 150 g toluene and 7.31 g 1-hexene (0.0870 mol). The polymerization was initiated by the addition of triethyl aluminum (0.1536 mmol) and tungsten hexachloride (0.0256 mmol) to the stock solution at 105 °C while the mixture was vigorously stirred for 1 h. The obtained toluene solution of the copolymer and 37.7 mg $RuHCl(CO)(PPh_3)_3$ as hydrogenation catalyst were mixed in an autoclave under a dry atmosphere. Then, the dry nitrogen in the autoclave was replaced by dry hydrogen. The mixture was allowed to heat to the hydrogenation temperature during stirring. Hydrogenation was carried out at 160 °C for 3 h under 10 MPa of H_2. The resulting viscous solution was poured into a large amount of methanol with vigorous stirring. The obtained white powder was dried at 100 °C under vacuum (yield = 96%). The procedure of homopolymer was carried out as well as copolymer synthesis (Scheme 1) [14].

Monomer reactivity ratio was determined by Fineman–Ross method as follows. Toluene/monomer feed ratio = 3, DCP/MMT wt% feed ratio in the range from 0.1, 0.3, 1, 3 and 9, initial temperature at 80, 105 and 130 °C, monomer/WCl_6 feed ratio = 30,000 and WCl_6/triethyl aluminum feed ratio = 6. The reaction solution was quenched by methanol within 10 s because monomer conversion should be depressed under 30%. DCP and MMT units incorporated into the copolymer were calculated by each monomer conversion.

2.3. Characterization

^1H NMR spectra were obtained using a Bruker AVANCE 500 MHz instrument using $CDCl_3$ as a solvent. GC measurement was conducted to determine monomer conversion with a Shimazu GC-2014 TC-WAX I.D. (0.53 mm length 30 m df 100 μm). Gel permeation chromatography (GPC) was performed in THF as an eluent using a TOSOH 8020 HPLC apparent equipped with four TSKgel columns (TSKgel G7000HxL, TSKgel GMHxL, TSKgel GMHxL and TSKgel G2000xL) using RI detector and polystyrene calibration. Thermal analysis was performed on a Seiko instruments DSC 6200 at a heating rate of 20 K/min. A chlorobenzene solution having a concentration of 5×10^{-3} g/cm^3 was prepared, and an intrinsic viscosity was measured under the condition of 30 °C using RIGOSHA & Co., Ltd, Automatic Viscometer VMC-222.

2.4. Preparation of polymer solution

Solutions for LS measurements were prepared by dissolving the appropriate amount of polymer in TL/CPE = 50/50 mixed solvent, TL/CHX = 50/50 mixed solvent, THF and dichloromethane (DCM) at seven concentrations of 0.2, 0.4, 0.6, 0.8, 5, 10 and 15 wt%. Solvents and polymer solutions were filtered through 0.2 and 0.5 μm PTFE filters, respectively, and measured directly into the scattering cell. The values of the refractive indexes n_0 at $\lambda_0 = 589$ nm of homopolymer and copolymer were 1.5120 and 1.5175, respectively. These values were close to that of TL (1.4960). Both polymers were not soluble in CHX and CPE. The measurements, therefore, in TL, CHX and CPE could not be carried out and mixed solvents consisting of TL and CHX, and TL and CPE were used.

2.5. Dynamic light scattering (DLS)

DLS measurements were carried out to determine D for four dilute solutions ($c = 0.2$, 0.4, 0.6, 0.8 wt%) of the homopolymer and the copolymer at four scattering angles of 60°, 90°, 120° and 150° at

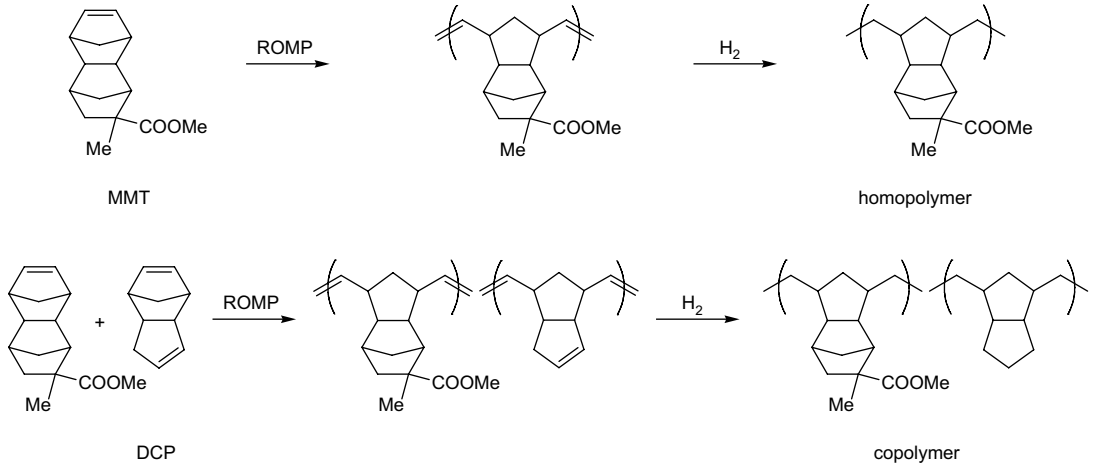

Scheme 1. Synthesis of homopolymer and copolymer.

Table 1
The monomer reactivity ratio of DCP and MMT

Reaction temp. (°C)	r_{DCP}	r_{MMT}	r_{DCP}/r_{MMT}
80	1.423	0.552	2.578
105	1.180	0.911	1.295
130	1.062	0.916	1.159

23 °C. In addition, we investigated the aggregation behavior of these two polymers in a dilute solution ($c = 0.8$ wt%) and three semi-concentrated solutions ($c = 5, 10, 15$ wt%) at a scattering angle of 60° at four temperatures of 23, 30, 40 and 50 °C. The measurements were made with an ALV/DLS/SLS-5000 light-scattering system, with a 22 mW He–Ne laser emitting vertically polarized light of 632.8 nm wavelength as the light source.

From the measurements, the normalized autocorrelation function $g_2(t)$ of scattered light intensity $I(t)$ at time t was measured:

$$g_2(t) = \frac{\langle I(0)I(t)\rangle}{\langle I(0)\rangle^2} \quad (1)$$

$g_2(t)$ is related to the normalized autocorrelation function $g_1(t)$ of the electric field by Siegert's relation [16]:

$$g_2(t) = 1 + \beta|g_1(t)|^2 \quad (2)$$

where β is a spatial coherence factor dependent on the detection system. For polydisperse solutes, $g_1(t)$ may be expressed by a continuous distribution function $G(\Gamma)$ of the decay rate Γ, which is the inverse of the decay time τ.

$$g_1(t) = \int_0^\infty d\Gamma\, G(\Gamma)\exp(-\Gamma t) \quad (3)$$

$G(\Gamma)$ leading to Γ was determined by performing an inverse Laplace transform on Eq. (3) from the data for $g_2(t)$ because the samples used in this study were polydisperse. This method is CONTIN analysis [17], which is useful for analysis of more complicated data. Because D is related to Γ in Eq. (4), D was determined by using Γ.

$$D = \Gamma/q^2 \quad (4)$$

q is the magnitude of the scattering vector

$$q = \frac{4\pi n_0}{\lambda_0}\sin\frac{\theta}{2} \quad (5)$$

defined in terms of the solvent refractive index n_0, the wavelength in vacuum of the light used λ_0, and the scattering angle θ. For dilute solutions, D may be expanded as

$$D = D_0(1 + k_D c + \cdots) \quad (6)$$

where D_0 is D at infinite dilution, and k_D is the diffusion second virial coefficient. The k_D could be a solubility index of polymers because k_D is related to the thermodynamic second virial coefficient A_2 [18]. The slope of each line divided by D_0 gives us k_D according to Eq. (6). From D_0, the hydrodynamic radius R_H is calculated by the Stokes–Einstein equation given in Eq. (7), with k_B Boltzmann constant, T the sample temperature, and η_0 the solvent viscosity.

$$R_H = \frac{k_B T}{6\pi\eta_0 D_0} \quad (7)$$

For semi-concentrated or concentrated solutions, two or more relaxation modes could be observed. These relaxation modes that involve the fast mode due to the motion of single polymer chain and the slow mode related to the motion of polymer aggregation in solution would be observed [19,20]. Note that the intensity of the fast mode is proportional to the osmotic compressibility and is strongly dependent on the solvent quality, while the slow mode corresponding to the elastic modulus is rather invariant with the solvent quality [21]. Unlike in the case of dilute solutions, correlation length x is calculated by using D on Eq. (8):

$$\xi = \frac{k_B T}{6\pi\eta_0 D} \quad (8)$$

Table 2
The copolymer composition of DCP and MMT[a]

	Conversion (%)		Copolymer composition[b] (wt%)	
	DCP	MMT	DCP	MMT
First stage	44.0	37.9	27.5	72.5
Final stage	96.2	93.7	25.5	74.5

[a] Monomer feed ratio DCP/MMT = 25/75 (wt%) at 105 °C as an initial internal temperature.
[b] Calculated by monomer conversion using GC.

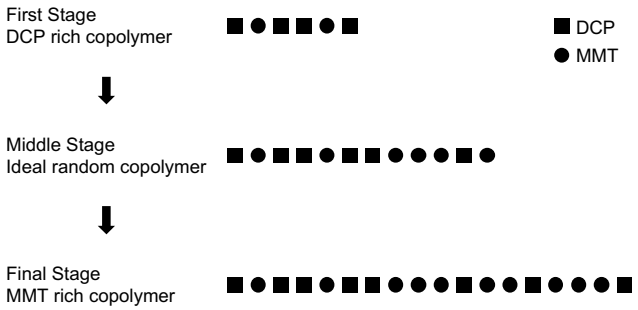

Scheme 2. Possible reaction mechanism of copolymer formation.

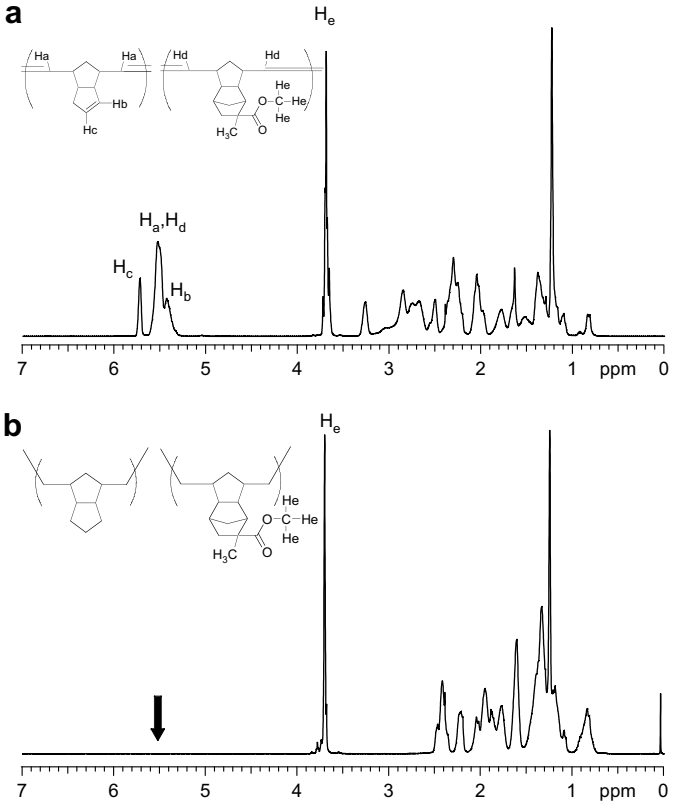

Fig. 1. (a) ^{1}H NMR spectrum of the copolymer before hydrogenation; (b) ^{1}H NMR spectrum of the copolymer after hydrogenation.

Table 3
Characterizations and properties of homopolymer and copolymer

Sample	Yield (%)	Molecular weight		M_w/M_n[b]	η[c]	MMT/DCP unit[d]		Degree of hydrogenation (%)	T_g[e] (°C)	Water absorption[f] (wt%)	Film withdrawing strength[g] (gf/100 μm)	Photoelastic coefficient (cm^2/dyn)
		M_w[a] (g/mol)	M_n[b] (g/mol)			Feed (wt%)	Found (wt%)					
Homopolymer	94	139,000	42,900	3.2	0.78	100/0	100/0	>99.9	171	0.4	17	3×10^{-12}
Copolymer	96	53,400	27,100	4.1	0.65	75/25	73.5/27.2	>99.9	148	0.2	42	3×10^{-12}

[a] Measured by SLS with THF solution.
[b] Measured by GPC using THF as eluent.
[c] Measured by intrinsic viscosity of 0.5 g/L in dichlorobenzene.
[d] Measured by ^{1}H NMR spectroscopy in $CDCl_3$.
[e] Measured by DSC.
[f] According to ASTM D570; water immersion at 23 °C for 2 weeks.
[g] Measured by K7128B.

In a narrow sense, ξ is not equal to R_H by definition. However, note that both physical values are shown together as R_H in the abscissa of some figures in order to compare the size of single polymer chain directly with that of aggregated polymer, and demonstrate the concentration dependence of polymer aggregation.

The refractive indices of the four solvents at 23 °C were determined with a Kyoto Electronics refractometer (model RA-500 N) to be 1.4558, 1.4547, 1.4057 and 1.4217, respectively. The densities of the four solvents at 23 °C were determined with a Kyoto Electronics density/specific gravity meter (model DA-505) to be 0.8141, 0.8131, 0.8842 and 1.3202 g/cm^3, respectively. The viscosity of the four solvents at 23 °C were determined with a Toki Sangyo rotational viscometer (model RE-80L) to be 0.468, 0.611, 0.491 and 0.468 cP, respectively. Applying polymer solution viscosity to size analysis of aggregate polymer might make the analysis more complicated because the amount of aggregate polymer depends on solution system. Therefore solvent viscosity was not used for size analysis of only single polymer chain but also aggregate polymer in Eqs. (7) and (8).

2.6. Static light scattering (SLS)

SLS measurements were carried out to determine the weight average molecular weight M_w and A_2 for four dilute solutions ($c = 0.2$, 0.4, 0.6, 0.8 wt%) of the homopolymer and the copolymer in the scattering angle range 30–150° at 10° intervals at 23 °C. The measurements were made with the same apparatus as DLS measurements. The values of $\partial n/\partial c$ for TL/CPE mixed solution, TL/CHX mixed solution, THF solution and DCM solution of the homopolymer at 23 °C were 0.0848, 0.0980, 0.1302 and 0.1135 cm^3/g, respectively. Meanwhile, the values of $\partial n/\partial c$ for the four solutions of the copolymer at 23 °C were 0.0850, 0.0938, 0.1358 and 0.1135 cm^3/g, respectively.

A_2 was calculated from the slope of concentration dependence at $\theta = 0$ in a Berry plot [22]:

$$\left(\frac{Kc}{\Delta R_{\theta=0}}\right)^{1/2} = \frac{1}{M_w^{1/2}}(1 + A_2 M_w c + \cdots) \tag{9}$$

where K is the optical constant

$$K = \frac{4\pi^2 n_0}{N_A \lambda_0^4}\left(\frac{\partial n}{\partial c}\right)^2 \tag{10}$$

defined in terms of n_0, the Avogadro number N_A, λ_0 and the refractive index increment $\partial n/\partial c$.

3. Results and discussion

3.1. Monomer reactivity ratio and synthesis of the copolymer

In order to investigate the copolymerization of MMT and DCP, the monomer reactivity ratio, i.e., r_{DCP}/r_{MMT}, was examined using

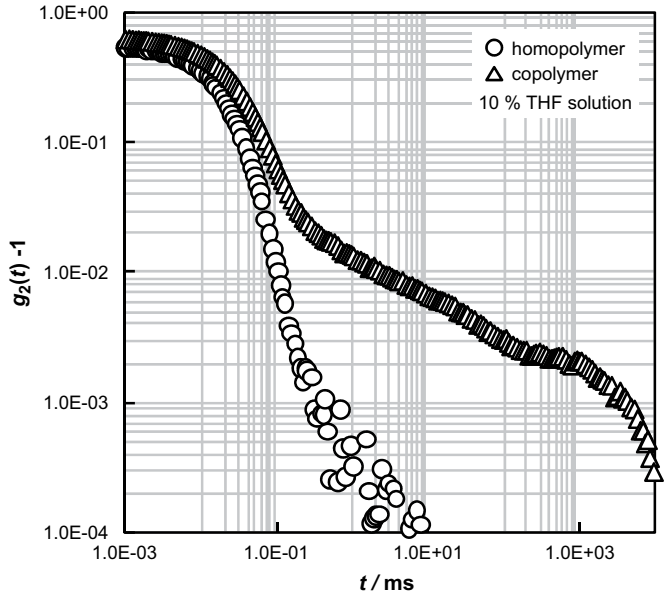

Fig. 2. Normalized autocorrelation functions of homopolymer and copolymer in THF solution with a concentration of 10 wt% at 23 °C and 60°.

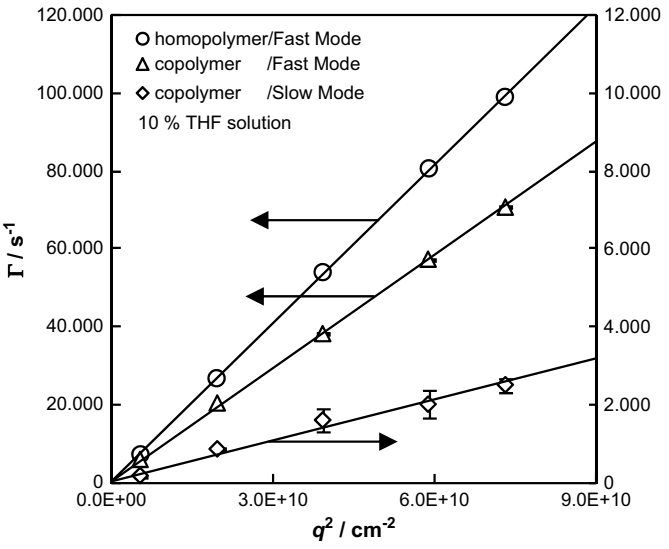

Fig. 3. Scattering vector (q^2) dependence of the decay rates (Γ) of homopolymer and copolymer in THF solution with a concentration of 10 wt% at 23 °C.

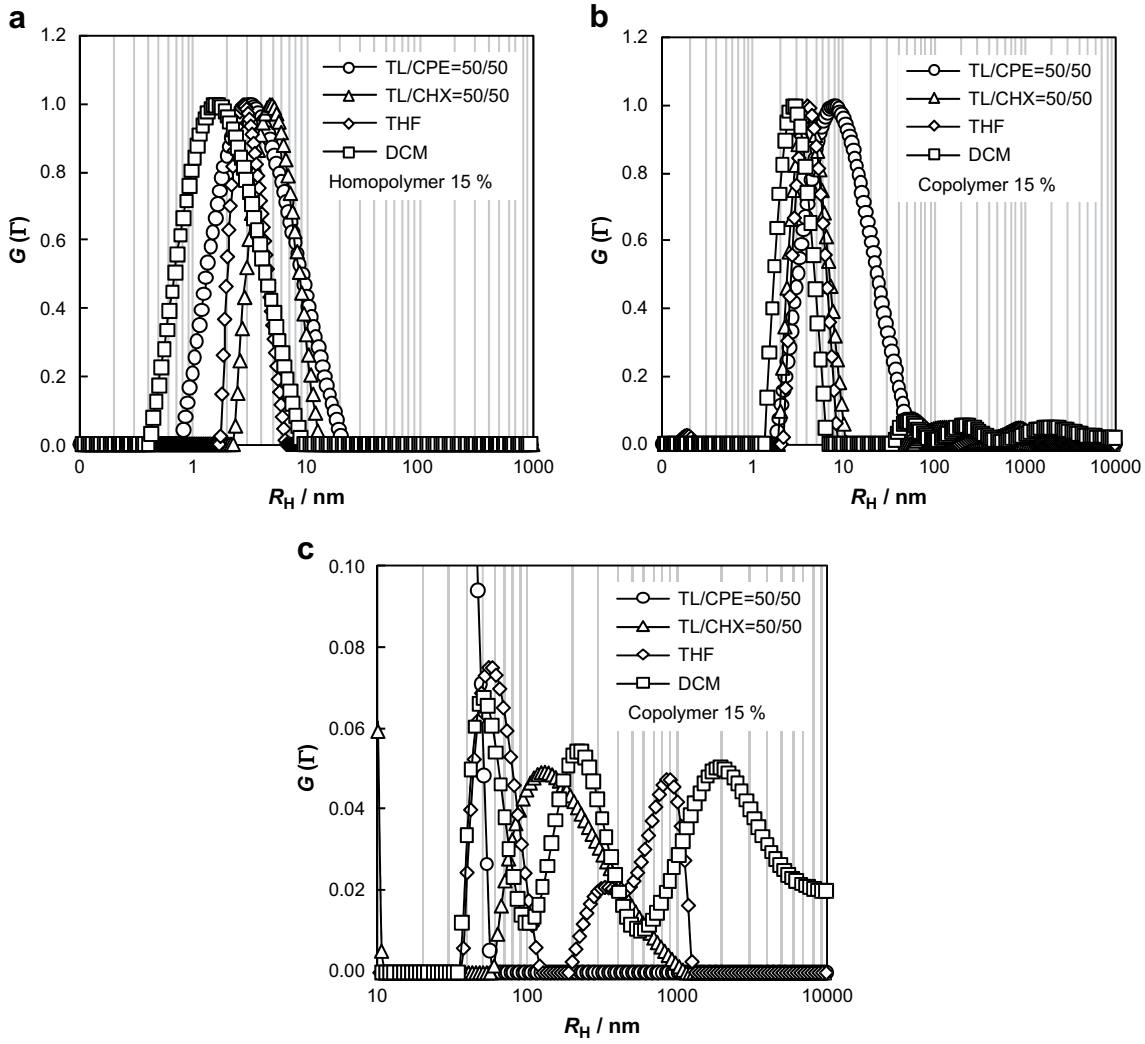

Fig. 4. (a) Decay rate distribution function versus the hydrodynamic radius of homopolymer in different four solutions with a concentration of 15 wt% at 23 °C and 60°; (b) decay rate distribution function versus the hydrodynamic radius of copolymer in different four solutions with a concentration of 15 wt% at 23 °C and 60°; (c) enlarged view of (b) in the hydrodynamic radius range from 10 to 10,000 nm.

Fineman–Ross method. The copolymerization of DCP and MMT was carried out in a temperature range from 80 to 130 °C.

As shown in Table 1, monomer reactivity of DCP was higher than that of MMT in any condition. With increasing reaction temperature, r_{DCP}/r_{MMT} decreased to approximately 1. The copolymerization without quenching at a DCP/MMT feed ratio = 25/75 wt% conducted at 105 °C as a start temperature was completed in 60 s. As a result, the internal final temperature of 140 °C could be attained to give the copolymer in 96% yield. Table 2 shows copolymer composition obtained at first stage and final stage.

Based on these findings, the reaction mechanism could be considered to be as follows: at first stage, DCP is incorporated into copolymer than the feed ratio. During the copolymerization, the internal temperature increased to give ideal random copolymer, i.e., $r_{DCP}/r_{MMT} = 1$, may be obtained. On the other hand, at final stage MMT rich copolymer was obtained because reactive DCP was almost consumed at this stage. That is, the copolymer structure had distribution of DCP unit in a macromolecule as shown in Scheme 2. This unique structure will provide interesting aggregation behavior, which will be discussed in the next section.

Fig. 1a shows ^{1}H NMR spectra of the final product obtained at 105 °C as initial temperature. The peaks at 5.30–5.80 ppm were assigned to vinyl protons of the copolymer main chain. To calculate the DCP unit incorporated into copolymer, the integrated intensity of DCP's single proton at 5.63 ppm (Hc) and MMT's three protons at 3.68 ppm (He) was used for this purpose. The amount of DCP unit was found to be high to the feed value because monomer reactivity ratio of DCP was higher than that of MMT.

Fig. 1b shows ^{1}H NMR spectra of the hydrogenated copolymer. In the hydrogenated copolymer, the presence of vinyl protons disappeared, which indicated that the main-chain double bonds were perfectly hydrogenated.

3.2. Practical properties of the copolymer

Table 3 shows the practical properties of the copolymer. For 27.2 wt% of DCP unit incorporated into copolymer, the glass transition temperature reduced from 171 to 148 °C and improved anti-water absorption and toughness because flexible DCP unit without polar methyl ester group was incorporated into polymer backbone. The amounts of water absorption of the homopolymer (0.4%) and the copolymer (0.2%) are very small compared with PMMA (1.93%). Photoelastic coefficients of both polymers (3.0×10^{-13} cm^2/dyn) are quite low compared with that of polycarbonate (80×10^{-13} cm^2/dyn) which is often used as an optical material. These results indicate that the copolymer with high withdrawing strength as well as good heat resistance offers interesting possibility for applications in optics as a thin tough optical film.

3.3. Aggregation behavior of the hydrogenated copolymer and homopolymer

The copolymer had both hydrophobic DCP units and hydrophilic MMT units and distribution of DCP unit in a macromolecule as discussed in previous section; therefore, it is very interesting to investigate its solution properties in various solvents with the aid of DLS and SLS measurements and compare to the homopolymer. Fig. 2 shows the DLS autocorrelation functions for the polar THF solutions of the homopolymer and the copolymer at concentrations of 10 wt%.

Only one relaxation mode (fast mode) is observed for the homopolymer; however, two relaxation modes (fast and slow modes) were observed for the copolymer. In order to reveal these two relaxation modes, the q^2 dependences of Γ for the THF solutions were examined as shown in Fig. 3.

Γ of all relaxation modes in both polymers are proportional to q^2, indicating that they are diffusive. It can be concluded, therefore, that the fast mode in each polymer is attributed to the diffusive motion of each single polymer chain, while the slow mode in the copolymer is caused by aggregated polymer. It is conceivable to assume that the homopolymer is homogeneously dissolved, while the copolymer is heterogeneously dissolved in THF, resulting in the polymer aggregation. Effects of solvent polarity and temperature on the aggregation of the copolymer were carried out to determine whether the selective depressions of the aggregation occurred or not. Fig. 4 shows the decay rate distribution functions for the TL/CPE mixed solutions, the TL/CHX mixed solutions, the THF solutions and the DCM solutions.

No polymer aggregates are detected in any of the four 15% solutions of the homopolymer (Fig. 4a) as well as the TL/CPE solution of the copolymer. The aggregates, however, are detected in the TL/CHX mixed solution, the THF solution and the DCM solution of the copolymer (Fig. 4b). It is worth noting that the aggregate peak for the TL/CHX mixed solution of the copolymer ranges from 50 nm to 1 μm, while the peaks for the THF solution as polar solvent and the DCM solution as polar solvent of the copolymer range from 30 nm to about 100 μm (Fig. 4c). These results indicate that the aggregation degree of the copolymer increases with solvent polarity. Fig. 5 shows the concentration dependence of the aggregate formation in the THF solution of the copolymer.

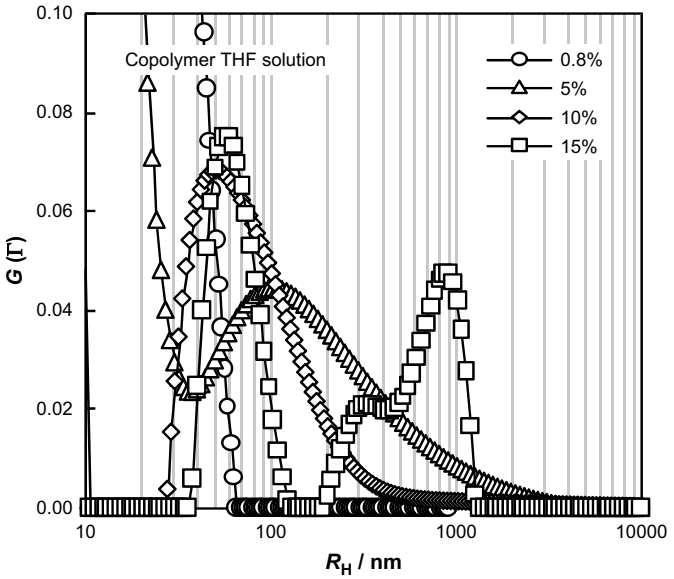

Fig. 5. Concentration dependence of the decay rate distribution function versus the hydrodynamic radius of copolymer in THF solution at 23 °C and 60°.

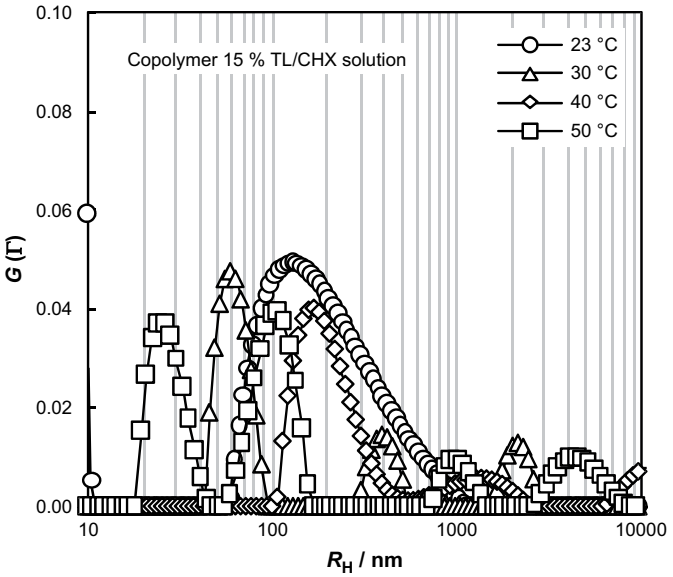

Fig. 6. Temperature dependence of the decay rate distribution function versus the hydrodynamic radius of copolymer in TL/CHX mixed solution with a concentration of 15 wt% at 60°.

It is interesting that the aggregate peak of the copolymer increases with concentration because solubility of the copolymer in high polar solvent decreases due to the low water absorption. This trend is also identified in the TL/CHX mixed solution and the DCM solution of the copolymer. Figs. 6 and 7 show the temperature dependences of aggregate formation in the TL/CHX mixed solution (Fig. 6) and THF solution (Fig. 7) of the copolymer, respectively.

With increasing temperature from 23 to 50 °C, the aggregate size decreased in the TL/CHX mixed solution as hydrophobic solvent, while no change was observed in the THF solution as polar solvent. In order to discuss the relations between the aggregate formation and the solubility of these two polymers, the dielectric constants ε of the four solvents, the peak area ratios of the aggregate peaks to all peaks in the four solution systems, the second

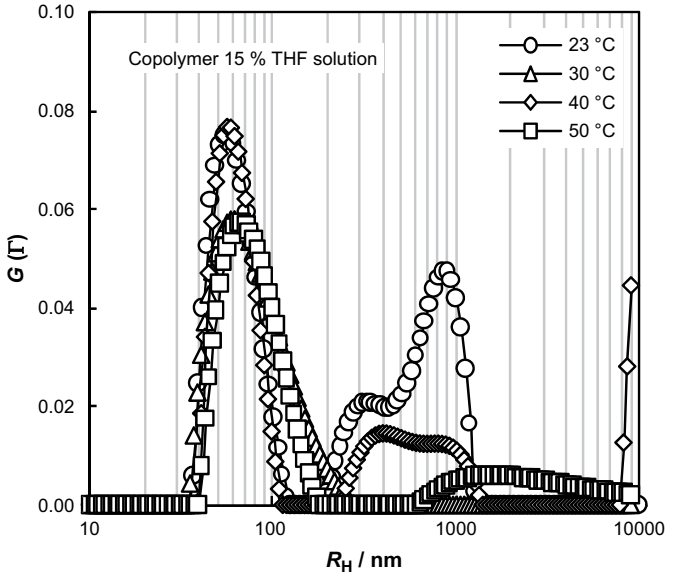

Fig. 7. Temperature dependence of the decay rate distribution function versus the hydrodynamic radius of copolymer in THF mixed solution with a concentration of 15 wt% at 60°.

Table 4
The relations between aggregation and solubility of homopolymer and copolymer

Solvent	ε (−)	Peak area of aggregation[a] (%)	$10^4 A_2$[a] (cm^3mol/g^2)	k_D[a] (cm^3/g)
TL/CPE = 50/50	2.23[b]	0.0/0.0	7.3/12.0	20.8/33.4
TL/CHX = 50/50	2.20[c]	0.0/7.2	8.1/12.0	20.2/30.0
THF	7.52[d]	0.0/12.4	9.6/8.1	55.4/13.5
DCM	8.93[d]	0.0/18.5	10.3/6.0	60.7/1.3

[a] Listed in the order corresponding to homopolymer/copolymer.
[b] The average value of TL (2.38) [23] and CPE (2.08) [23].
[c] The average value of TL (2.38) [23] and CHX (2.02) [23].
[d] The value of literature [23].

virial coefficients A_2 and the diffusive second virial coefficients k_D are shown in Table 4. Note that A_2 and k_D are due to single mode because copolymer was not also confirmed to aggregate in dilute solutions.

As for the copolymer, the peak area ratios of the polymer aggregation increase, and A_2 and k_D corresponding to the polymer solubility decrease with increasing solvent polarity. Because the fast mode detected by DLS is strongly dependent on the solvent properties, k_D changes more significantly than A_2 on increasing the solvent polarity. Meanwhile, as for the homopolymer, no polymer aggregates are formed, and A_2 and k_D increase with increasing the solvent polarity. Based on these findings, it is concluded that in poor solvents such as THF and DCM, hydrophobic DCP-rich units in a macromolecule may aggregate with DCP as the core unit. It is also interesting to compare the result of the TL/CPE mixed solution with that of the TL/CHX mixed solution. Both CPE and CHX are cyclic hydrocarbon solvents but the polymer aggregation behaviors in these two mixed solutions with the addition of TL are different from each other. The polymer aggregate is not formed in the TL/CPE mixed solution but is formed in the TL/CHX mixed solution. CPE, which has smaller size than CHX, may penetrate into the polymer and depress aggregate formation.

4. Conclusion

New cyclic saturated homopolymer and copolymer were prepared from MMT and DCP via ROMP. Kinetic studies indicate that a copolymer has distribution of DCP unit in a macromolecule. The distribution causes the copolymer to aggregate with DCP as the core unit in poor solvents such as THF and DCM; on the other hand, using TL/CPE mixed solvent or TL/CHX mixed solvent with an elevated heating temperature can prevent aggregation.

Acknowledgement

We are deeply grateful for the useful discussions with Prof. Takenao Yoshizaki (Kyoto University), Dr. Shin-ichi Kimura, Dr. Zen Komiya and Mr. Ichirou Kajiwara (JSR Corporation).

References

[1] Katime I, Quintana J. Makromol Chem 1986;187:1441–55.
[2] Topouza D, Orfanou K, Pispas S. J Polym Sci Part A Polym Chem 2004;42:6230–7.
[3] Zhou J, Zhang L. Polym J 2000;32:866–70.
[4] Petzold K, Klemm D, Heublein B, Burchard W, Savin G. Cellulose 2004;11:177–93.
[5] Tsunashima R. Kobunshi Kako 2003;52:242–9.
[6] Nolan D, Darcy R, Ravoo B. Langmuir 2003;19:4469–72.
[7] Chaibundit C, Ricardo N, Crothers M, Booth C. Langmuir 2002;18:4277–83.
[8] Liaw D, Huang C, Sang H, Kang E. Polymer 2001;42:209–16.
[9] Virtanen J, Arotcarena M, Heise B, Ishana S, Laschewsky A, Tenhu H. Langmuir 2002;18:5360–5.
[10] Bakeev K, Shu Y, Zein A, Kabanov V, Lezov A, Mel'nikov A, et al. Macromolecules 1996;29:1320–5.
[11] Wang C, Tam K, Jenkins R. J Phys Chem B 2002;106:1195–204.
[12] Rubio L, Castillo OM, Rejon L, Olayo R, Cruz G. J Polym Sci Part B Polym Phys 2002;40:2130–6.
[13] Kwan S, Hu Q, Ma L, Pu L, Wu C. J Polym Sci Part B Polym Phys 1998;36:2615–22.
[14] Yoshida Y, Goto K, Komiya Z. J Appl Polym Sci 1997;66:367–75.
[15] Yoshida Y, Yoshinari M, Ito A, Komiya Z. Polym J 1998;30:819–23.
[16] Siegert A. J MIT Radiat Lab Rep; 1942.
[17] Provencher SW. J Chem Phys 1976;64:2772–7.
[18] Yamakawa H. J Chem Phys 1962;36:2995–3001.
[19] Brochard F, de Gennes PG. Macromolecules 1977;10:1157–61.
[20] Adam M, Delsanti M. Macromolecules 1985;18:1760–70.
[21] Stepanek P. Macromolecules 1998;31:1889–97.
[22] Berry GC. J Chem Phys 1966;44:4550–64.
[23] Lide DR. Handbook of organic solvents. Boca Raton; FL: CRC Press; 1995.